A cost-effective WDM-PON architecture simultaneously supporting wired, wireless and optical VPN services

Yanzhi Wu, Tong Ye *, Liang Zhang, Xiaofeng Hu, Xinwan Li, Yikai Su

State Key Lab of Advanced Optical Communication Systems and Networks, Shanghai Jiao Tong University, Shanghai 200240, China

ARTICLE INFO

ABSTRACT

It is believed that next-generation passive optical networks (PONs) are required to provide flexible and various services to users in a cost-effective way. To address this issue, for the first time, this paper proposes and demonstrates a novel wavelength-division-multiplexed PON (WDM-PON) architecture to simultaneously support three types of services: 1) wireless access traffic, 2) optical virtual passive network (VPN) communications, and 3) conventional wired services. In the optical line terminal (OLT), we use two cascaded Mach–Zehnder modulators (MZMs) on each wavelength channel to generate an optical carrier, and produce the wireless and the downstream traffic using the orthogonal modulation technique. In each optical network unit (ONU), the obtained optical carrier is modulated by a single MZM to provide the VPN and upstream communications. Consequently, the light sources in the ONUs are saved and the system cost is reduced. The feasibility of our proposal is experimentally and numerically verified.

1. Introduction

Next-generation passive optical networks (PONs) are expected to provide diverse services to end users [1–5]. Firstly, a PON capable of supporting wireless service has been considered as a promising technique to significantly increase the coverage area of wireless access networks and reduce the system overall cost, because of the huge bandwidth and low attenuation offered by optical fiber [1–3]. Secondly, there are increasing demands to support high-speed private communications (e.g., video conference) among the end users in the LANs connected to different optical network units (ONUs) in a single PON [4,5]. Thus, a PON that can simultaneously support the above mentioned services in addition to the conventional downstream and upstream wired transmissions will be very attractive.

Several PON architectures have been developed to support either wireless access or high-speed inter-communications among the ONUs. The wavelength-division-multiplexed PON (WDM-PON) reported in Ref. [6–8] transports radio-frequency (RF) signals, such that the capacity, coverage area, and mobility of the access networks can be largely increased. However, these schemes do not consider private communications among the ONUs. Optical-layer virtual private network (OVPN) proposed in Ref. [4,5,9–11], implementing all-optical inter-connections among the ONUs, is an effective approach to meet various services demand, which can remarkably increase the network throughput, reduce the transmission latency,

and enhance the ONU-communication security [9]. However, such kind of PON structures does not support wireless access.

For the first time to the best of our knowledge, we propose and experimentally demonstrate a cost-effective WDM-PON structure using orthogonal modulation technique, to provide wireless, optical VPN, and conventional wired downstream and upstream services simultaneously. Compared with previous works [6,7], our scheme can provide more types of services while does not require more electrical and optical devices. In the OLT, we use two cascaded Mach–Zehnder modulators (MZMs) for each wavelength channel to generate an optical signal containing three frequency components. The double side-band frequency components carry the wireless traffic and the downstream data through the orthogonal modulation. The optical carrier in the center is sent to the ONU and modulated by an MZM for the purpose of the VPN and upstream communications, such that the ONU can be source-free and the system cost can be reduced.

2. Principle and architecture

The proposed architecture of WDM-PON enabling optical VPN is depicted in Fig. 1. At the optical line terminal (OLT), for each WDM channel, the output of a continuous wave (CW) laser is split into two parts. The first part of the CW light is modulated by two MZMs to generate the conventional downstream wired traffic and the wireless data. The first MZM biased at its null point is driven by a bipolar data mixed with a radio-frequency (RF) carrier, to generate an optical carrier suppressed-differential phase-shift keying (OCS-DPSK) signal for conventional wired communication. To load the wireless traffic, the intensity of the OCS-DPSK signal is modulated by the second MZM,

* Corresponding author. Tel.: +86 2134204602; fax: +86 2134204370.
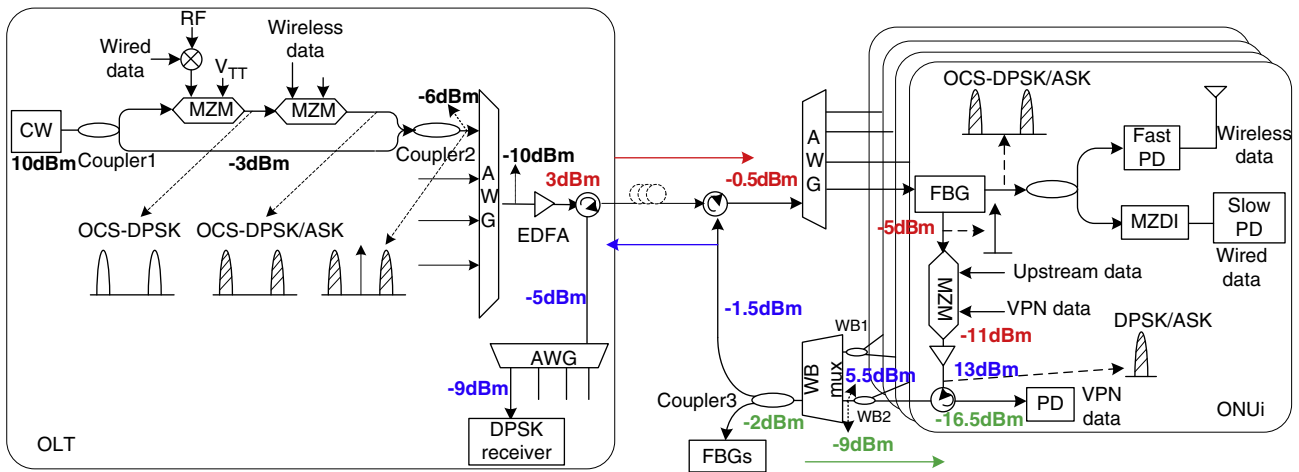 *E-mail address:* yetong@sjtu.edu.cn (T. Ye).

Fig. 1. The architecture of WDM-PON enabling optical VPN.

which generates an OCS-DPSK/ASK signal. The extinction ratio (ER) of the ASK modulation is set low such that the information loaded by the phase modulation in the first MZM can be maintained. The second part of the CW light from the laser does not experience the modulation, and is combined with the first part through a coupler. The combined signals on different wavelength channels are multiplexed together by an arrayed waveguide grating (AWG) to construct a WDM signal.

On the ONU side, the WDM signal is demultiplexed by an AWG. For each wavelength channel, a fiber Bragg grating (FBG) is used to separate the optical carrier and OCS-DPSK/ASK signal. The OCS-DPSK/ASK signal is divided into two parts. The first part is directly detected by a fast photo detector (PD) to recover the wireless ASK signal, while the second part is demodulated by a Mach–Zehnder delay interferometer (MZDI) and then detected by a slow PD to obtain the downstream data. The reflected optical carrier is modulated by a MZM biased around its null point to obtain a DPSK signal for the upstream transmission. The VPN data are superimposed onto the DPSK signal to form ASK/DPSK format by modulating the bias point between the null point and a small fraction of switching voltage [10]. This modulation technique is referred to as orthogonal modulation, since both the amplitude and the phase of the carrier are modulated. In this way, one can save a light source in each ONU, which reduces the system cost.

To support all-optical inter-connections among the ONUs, the ONUs at the adjacent wavelength channels in a same waveband (WB) are grouped to form an optical VPN [11]. The signal carrying the upstream and VPN data are split into two parts by a 1×2 coupler. One part is directly transmitted to the OLT through a circulator, while the other part is reflected by a fiber Bragg grating (FBG) next to the coupler and broadcasted within the VPN. The VPN data are directly received by a PD in the ONU. Note that, the ONUs in each VPN should send their VPN traffic in a time-division multiplexed (TDM) manner.

Herein, we consider the power budgets for the upstream and VPN transmissions, since the upstream and VPN signals pass through a lot of optical passive components before reach the destinations. The optical carrier for the upstream and VPN transmissions is remotely provided by the OLT. According to the typical insertion loss of the commercial components listed in Table 1 and the schematic setup in Fig. 2, the power of the optical carrier is − 10 dBm after the AWG on

the OLT side, if the output power of the laser is 10 dBm. This implies that the amplification is indispensable to ensure that the optical carrier can be employed by the ONU. Suppose that a WDM-PON has 16 wavelength channels in the system [12] and the saturated output power of a commercial EDFA is 18 dBm. It follows that the power of the optical carrier at each wavelength channel after the EDFA can reach 3 dBm. The amplified optical carrier is transmitted over a 12.5-km single mode fiber (SMF), demultiplexed by the AWG in the remote node, and then filtered out by an FBG on the ONU side, which results in a power loss of 8 dB. To carry the upstream and VPN data, the optical carrier is modulated by the MZM with an insertion loss of 6 dB. Hence, the signal power at the output of the MZM is about − 11 dBm. We thus use an EDFA with a gain of 24 dB to amplify this signal. Assume that a VPN typically contains 5 ONUs [13], and a 1×5 coupler with an insertion loss of 7 dB is employed for each VPN. Consequently, the power of the upstream and VPN signals are − 9 dBm and − 16.5 dBm when they reach the respective receivers. If one uses a 2.5-GHz PIN with a sensitivity of − 24 dBm for detection, the power margins for the upstream and VPN signals are 15 dB and 7.5 dB, respectively.

3. Experiment and simulation

To verify the principle of the proposed WDM-PON structure, we perform simultaneous transmission of the conventional wired traffic, the wireless data, as well as the VPN internetworking.

Fig. 2 depicts the experimental setup. A CW light is divided into two parts by a 95:5 coupler. We feed the 95% part to the upper branch, taking into consideration the insert loss of the two MZMs. The first MZM biased at its V_π (~ 7.2 V) is driven by a 1.25-Gb/s pseudorandom bit sequence (PRBS) data of 2^7-1 mixed with a 10-GHz RF signal to generate OCS-DPSK signal. The eyediagram of the mixed electrical signal, the spectrum and the eyediagram of the obtained optical signal are shown in Fig. 2, respectively, as insets (i), (ii) and (iii). The inset (ii) of Fig. 2 indicates the carrier suppression ratio is larger than 18 dB, which is recorded by an optical spectrum analyzer (Anritsu MS9710B) with a resolution of 0.07 nm. The output OCS-DPSK signal is modulated by the second MZM driven with another 1.25-Gb/s PRBS data. The spectrum, waveform and eyediagram of the output signal

Table 1
Typical insertion loss

Device	MZM	AWG	12.5-km SMF	Circulator	WB MUX	95:5 Coupler 1	3-dB coupler 2 and coupler 3	FBG
Insertion loss (dB)	6	4	2.5	0.5	4	13	3	0.5
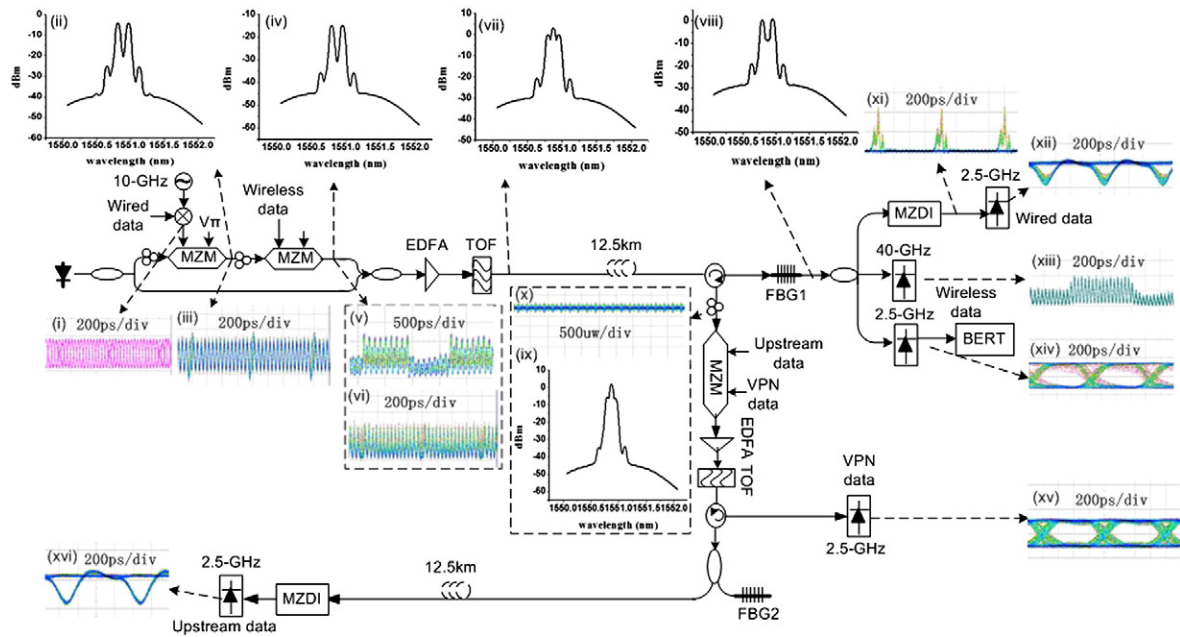
Fig. 2. Experimental setup and results. (i) The eyediagram of mixed electrical signal; (i) and (iii) the spectrum and the eyediagram of the OCS-DPSK signal; (iv), (v) and (vi) the spectrum, the waveform and the eyediagram of OCS-DPSK/ASK signal; (vii) the spectrum of amplified signal containing optical carrier and sub-carriers; (viii), (ix) and (x) the optical spectral of the passing part and reflected part of signal after FBG1, and the optical eyediagram of the reflected optical carrier; (xi) and (xii) the eyediagram of OCS-DPSK/ASK signal after MZDI and PD; (xiii) the waveform of received wireless data; (xiv), (xv) and (xvi) the eyediagrams of three types of data.

are given in insets (iv), (v) and (vi) of Fig. 2. The extinction ratio of ASK signal is adjusted to 2:1 to maintain the phase information, as shown in the inset (v) of Fig. 2. The produced OCS-DPSK/ASK signal coupled with the optical carrier is amplified to 4 dBm, and a tunable optical filter (TOF) with a bandwidth of 0.4 nm is used to suppress the amplified spontaneous emission (ASE) noise. The spectrum of the signal after TOF is shown in Fig. 2 (vii).

After transmission over 12.5-km SMF, the OCS-DPSK/ASK signal and the optical carrier are separated by FBG1, which has a 3-dB bandwidth of 0.106 nm and a reflection ratio of 90%. The spectral of passing part and reflected part are provided in Fig. 2 as insets (viii) and (ix). Inset (x) of Fig. 2 shows that the reflected optical carrier has a 10-GHz clock component due to the nonideal optical filtering. The clock component will disappear if: (a) an FBG with a higher reflection ratio and narrower bandwidth were employed, and (b) the distance between the sidebands and the carrier is increased. In Fig. 3, our simulation results obtained by VPI software show that the filtered

optical carrier has almost no fluctuation, if the frequency distance between the carrier and the sidebands is higher than 20-GHz. We expect that our scheme will perform very well when it is used in the 60-GHz system, which has attracted a growing interest because of its 7-GHz license-free bandwidth [14].

3.1. Results of downstream transmission

The OCS-DPSK/ASK signal is split into three parts. Due to the lack of a commercial MZDI, the first part is demodulated by a home-made 8-GHz MZDI and then received by a 2.5-GHz PD to obtain the downstream data. The downstream signal consists of two frequency components, which carry the same DPSK data. Such an OCS-DPSK is injected into a MZDI for phase-to-intensity conversion [15]. After the MZDI, the OCS-DPSK signal is converted to an OCS-ASK signal. Fig. 2 (xi) gives the waveform of the OCS-ASK signal, which clearly contains a 20-GHz frequency component. This can be explained as follows.
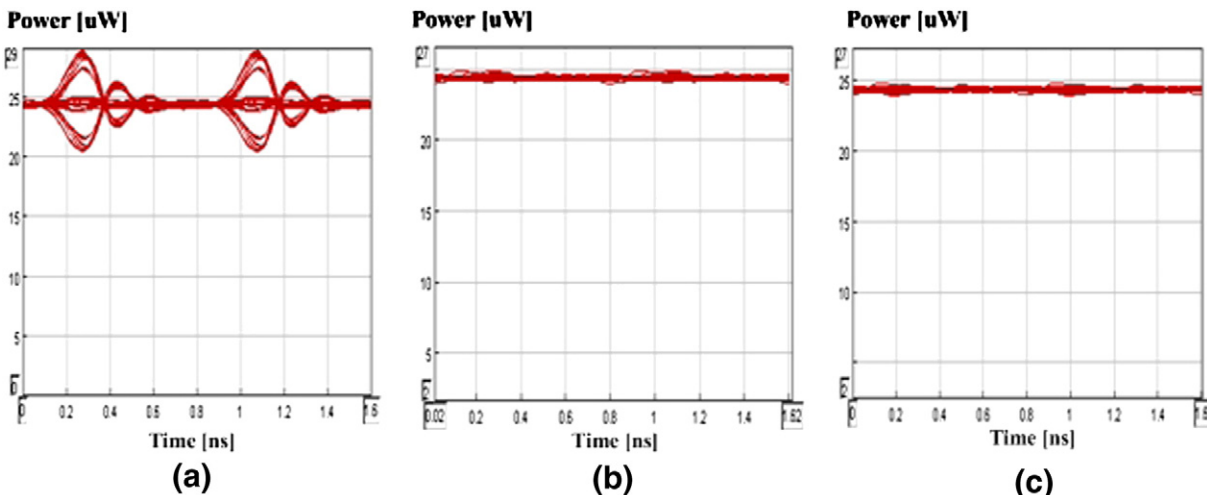
Fig. 3. The eyediagram of filtered optical carrier when the frequency of the RF signal is: (a) 10-GHz, (b) 20-GHz, (c) 30-GHz.

When such an OCS-ASK signal is fed to the oscilloscope (HP_Agilent 83480A), its two identical ASK components beat with each other at the 40-GHz PD equipped in the oscilloscope, which generates an ASK signal containing a 20-GHz frequency component. To recover the baseband waveform, we use a 2.5-GHz PD to remove the high-frequency components. Fig. 2(xii) shows that the recovered baseband signal has a good quality. The bit-error-rate (BER) performance of the downstream data before (see B-t-B in the figures) and after the 12.5-km transmission is compared in Fig. 4a, which indicates that the penalty is less than 1 dB. Notice that the quality of the downstream data is sensitive to the temperature and vibration since the employed MZDI is home made. If a commercial MZDI were available, the quality of the downstream signal can be improved significantly.

The second part is directly detected by a 40-GHz PD, and its waveform in inset (xiii) of Fig. 2 confirms that the wireless signal, 20-GHz RF carrier carrying a 1.25-Gb/s ASK signal, can be successfully received after the transmission. The eyediagram and the BER performance of the 1.25-Gb/s wireless data are provided in inset (xiv) of Figs. 2 and 4b, respectively. These results are obtained by directly detecting the third part using a 2.5-GHz PD, due to the lack of a high-speed electrical mixer. We note that, in practice, the 20-GHz wireless signal should be down-converted to baseband by frequency mixing [16] for data receiving at the user side. To verify the feasibility of our scheme, we conduct the simulation using VPI software. Fig. 5a and b show that the difference between the eyediagrams without and with the electrical mixer is small. The Q-factors of the recovered signals based on direct detection and down-conversion schemes are 13.3 and 11.2, respectively, when the received signal power is −21 dBm. Also, the BER performances in Fig. 5c and d indicate that the power penalty introduced by the electrical mixer is about 1.7 dBm.

3.2. Results for upstream and VPN transmissions

The optical carrier filtered by FBG1 is orthogonally modulated according to our principle mentioned in Section 2 to simultaneously carry the 1.25-Gb/s DPSK data and the 1.25-Gb/s ASK signal to support the traditional upstream and the VPN communications. However, its implementation in the experiment requires a high-power RF driver such that the voltage swing of the driving signal can reach $2V_\pi$. We explain this as follows. If the RF voltage swing is less than $2V_\pi$ and the VPN data are in the state of bit 0, as shown in Fig. 6a and b, the MZM driven by a bipolar upstream data is biased at V_π, and a standard DPSK signal is produced. When the VPN data change to the state of bit 1, the MZM driven by the upstream data is biased at $V_\pi \pm \Delta V$, and generates a DPSK signal having an amplitude fluctuation, as plotted in Fig. 6b. As a result, the output optical DPSK/ASK signal will have multiple levels, which will remarkably increase the complexity of the signal detection at the receiver. However, if the RF voltage swing is equal to $2V_\pi$, the undesired amplitude fluctuation disappears and a good DPSK/ASK signal can be obtained by the above-mentioned orthogonal modulation technique (see Fig. 6c and d). We perform a simulation by VPI software to verify the DPSK/ASK orthogonal modulation scheme using a single MZM. In the simulation the drive voltage at RF port is $2V_\pi$ and the bit-rate of the upstream and VPN signals are both 1.25-Gb/s. Fig. 7a is the output optical eyediagram after orthogonal modulation. We can see it has two amplitude levels, consisting with what we explained in Fig. 6c and d. After a 2.5-GHz PD, the ASK signal is recovered and its electrical eyediagram with a good eye-opening is depicted in Fig. 7b. The DPSK signal is received by a 1.25-GHz MZDI followed by a 2.5-GHz PD, and the output eyediagrams in Fig. 7c and d show that the DPSK signal can be successfully received. However, in
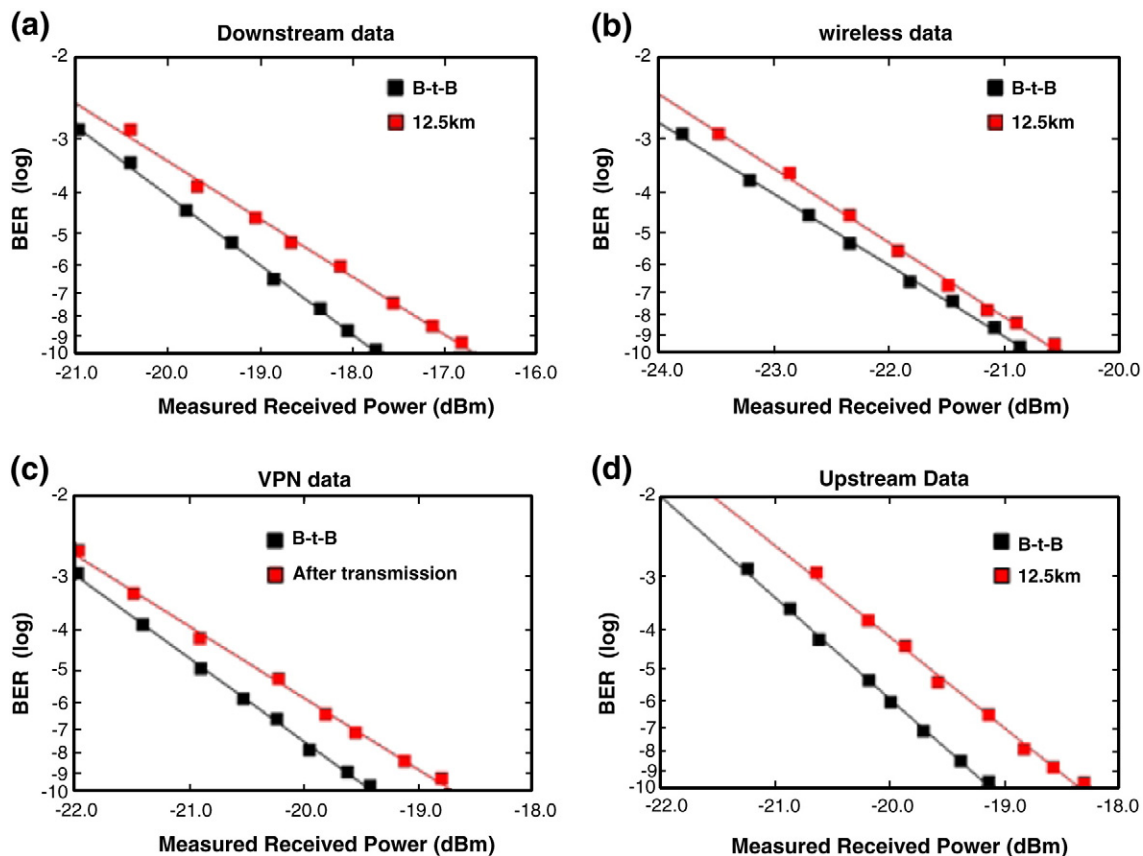

Fig. 4. BER curves for (a) downstream data, (b) wireless data, (c) VPN data, and (d) upstream data, where B-t-B is the short for back to back.
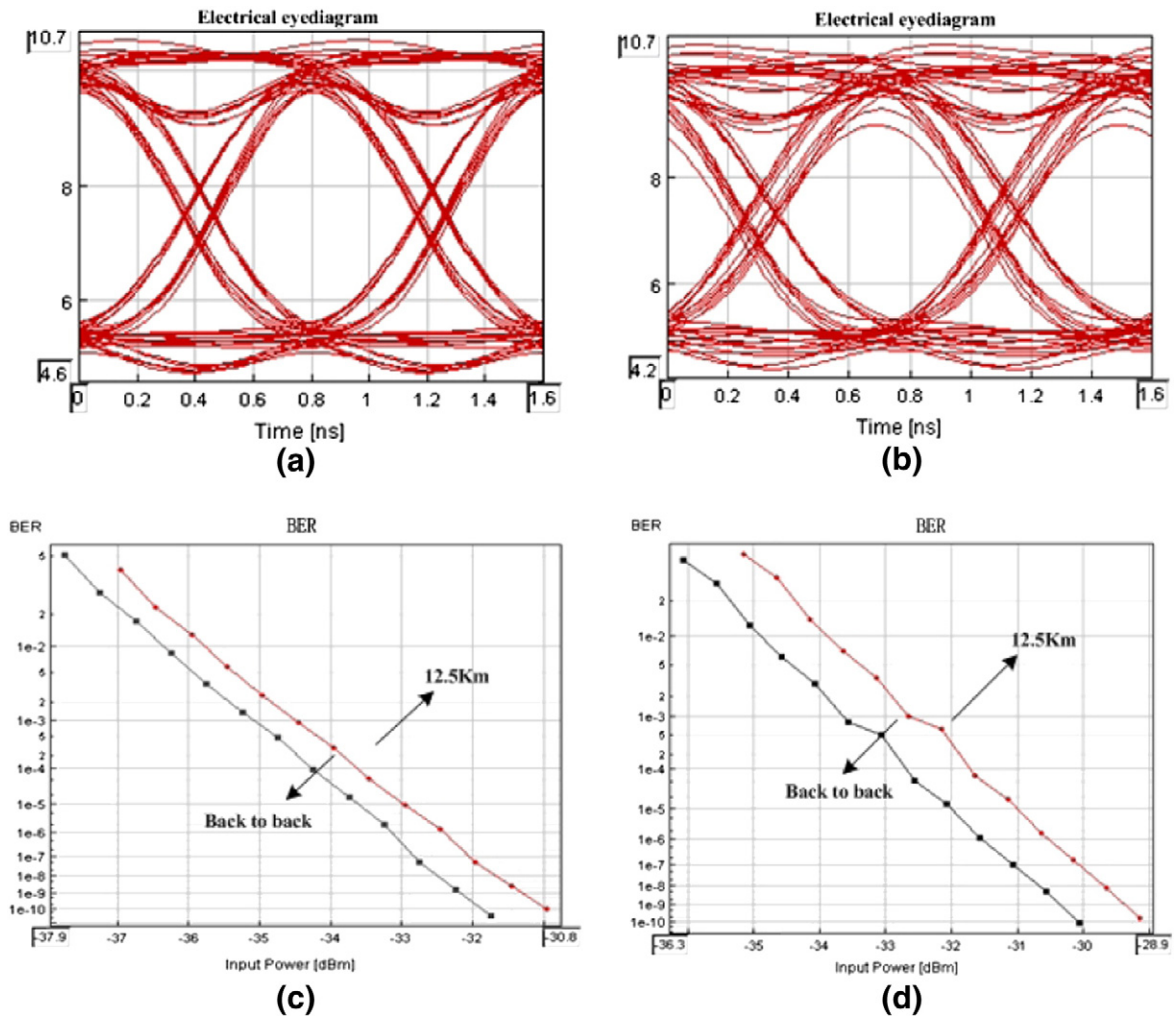
Fig. 5. Simulation results: electrical eyediagrams and BER curves with different detection methods: (a) and (c) direct detection without a mixer; (b) and (d) using the method with a mixer for down-conversion in Ref. [14].
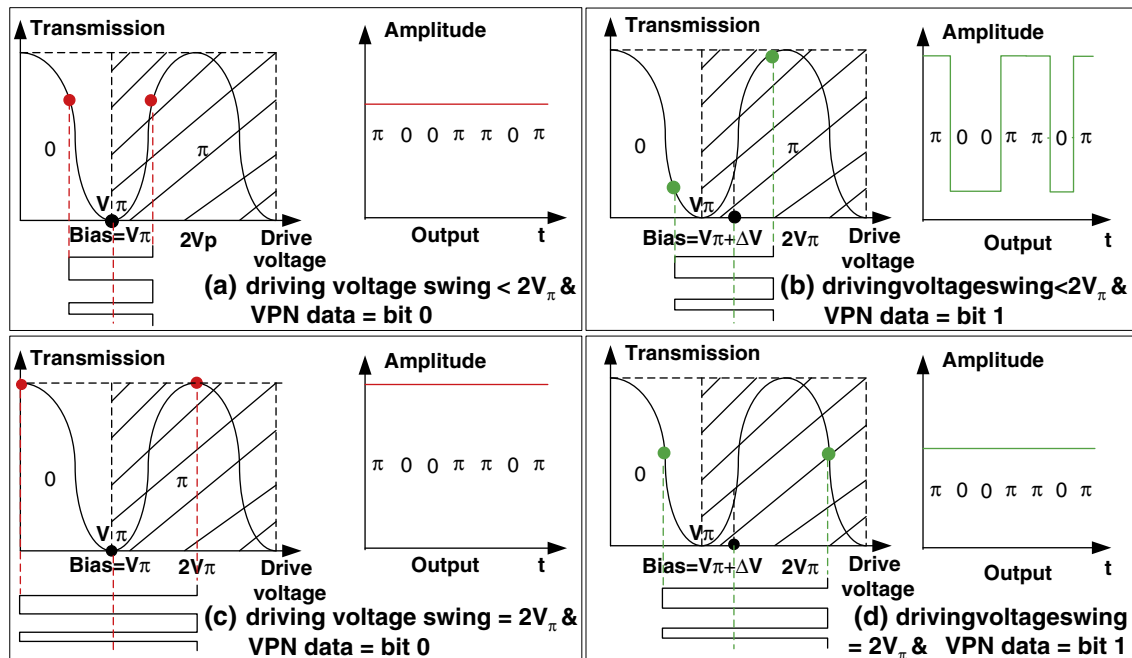

Fig. 6. Orthogonal modulation using a signal MZM: The driving voltage swing is less than $2V_\pi$ and (a) the VPI data are in the state of bit 0 or (b) bit 0; the driving voltage swing is equal to $2V_\pi$ and (c) the VPI data are in the state of bit 0 or (d) bit 0.
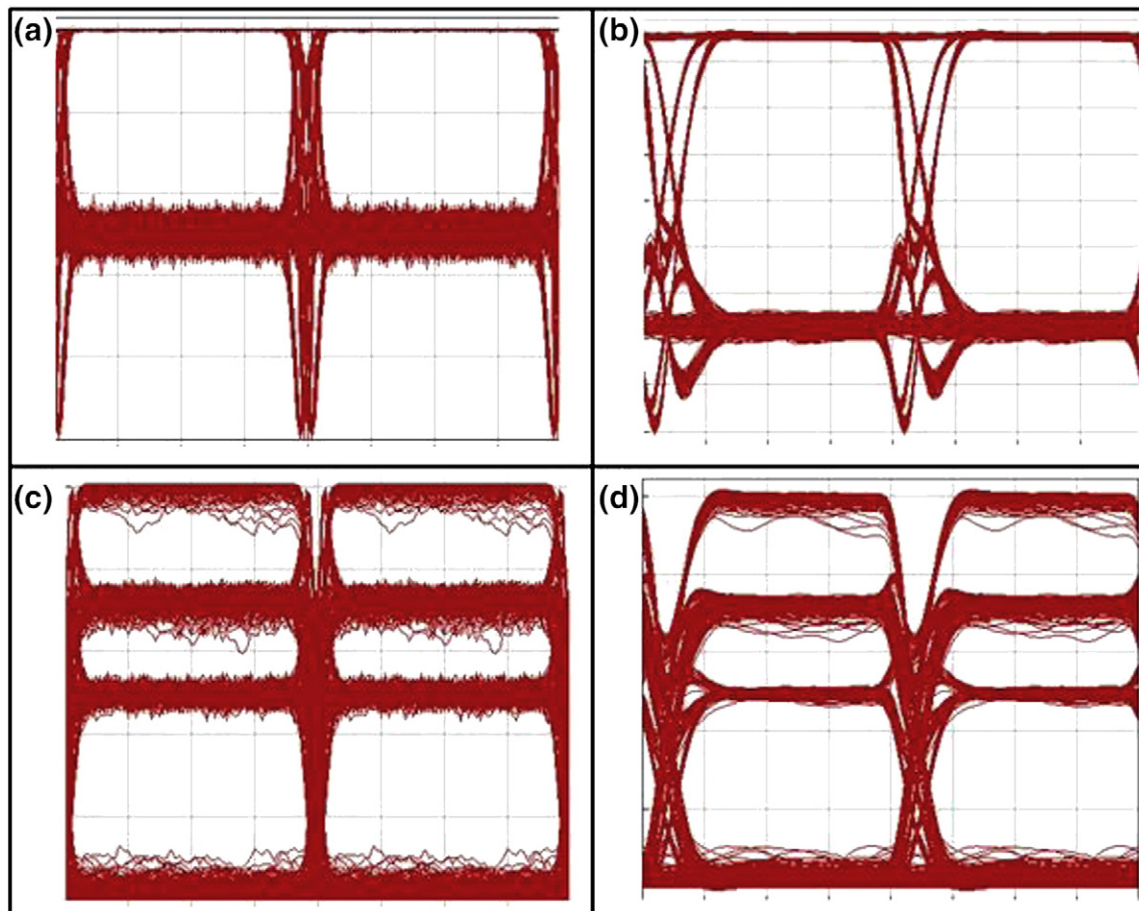
Fig. 7. Simulation results for orthogonal modulation using one MZM. Eyediagrams (200 ps/div): (a) signal after orthogonal modulation, (b) signal after 2.5-GHz PD direct detection, (c) and (d) signal after 1.25-GHz MZDI demodulation and then received by 2.5-GHz PD.

our experiment, these two kinds of data are modulated separately in interleaved time slots, because the employed modulator RF driver cannot provide an output swing of $2V_{\pi}$.

After the carrier is modulated by the MZM, the output signal is divided to two parts by a 3-dB coupler. One part is reflected back by the FBG2 with the same parameters as the above-mentioned FBG1, for the purpose of the VPN communication. A 2.5-GHz PD is used to receive the VPN data, whose eyediagram is displayed in inset (xv) of Fig. 2. Fig. 4c indicates that the VPN transmission penalty is about 0.6 dB. The second part is transmitted to the OLT, and a DPSK receiver is used to recover the upstream data. Both the eyediagram in Fig. 2 (xvi) and the BER curve in Fig. 4d verify that the upstream communication is feasible.

4. Conclusion

We propose a cost-effective WDM-PON structure to simultaneously support wired, wireless and optical VPN services. The OLT can generate the downstream data, wireless traffic and an optical carrier on each wavelength channel by employing two cascaded MZMs, while each ONU can support the upstream and the OVPN communications with only one MZM by utilizing the optical carrier remotely provided by the OLT. Our experimental demonstrations indicate that this simple and cost-effective scheme can be used in next-generation PON to provide flexible and various services to the end users.

Acknowledgement

References

[1] Gee-Kung Chang, Arshad Chowdhury, Zhensheng Jia, Hung-Chang Chien, Ming-Fang Huang, Jianjun Yu, Georgios Ellinas, Key technologies of WDM-PON for future converged optical broadband access networks [invited], j. Opt. Commun. Netw. 1 (4) (2009) C35.

[2] C.W. Chow, C.H. Yeh, Advanced modulation formats for delivery of heterogeneous wired and wireless access networks, Opt. Commun. 282 (2009) 4688.

[3] Jianqiang Li, Xu. Kun, Yang Jing Wen, Fu. Songnian, Ming Tang, Ping Shum, Wu. Jian, Jintong Lin, Experimental demonstration of polarization multiplexing for simultaneously providing broadband wireless and wired access, Opt. Commun. 281 (2008) 2806.

[4] C.-J. Chae, L. Seung-Tak, K. Geun-Young, P. Heesang, A PON system suitable for internetworking optical network units using a fiber Bragg grating on the feeder fiber, IEEE Photon. Technol. Lett. 11 (12) (1999) 1686.

[5] Nishaanthan Nadarajah, Manik Attygalle, Ampalavanapillai Nirmalathas, Elaine Wong, A novel local area network emulation technique on passive optical networks, IEEE Photon. Technol. Lett. 17 (5) (2005) 1121.

[6] Shu-Hao Fan, Hung-Chang Chien, Yu-Ting Hsueh, Arshad Chowdhury, Jianjun Yu, Gee-Kung Chang, Simultaneous transmission of wireless and wireline services using a single 60-GHz radio-over-fiber channel by coherent subcarrier modulation, IEEE Photon. Technol. Lett. 21 (16) (2009) 1127.

[7] Zizheng Cao, Jianjun Yu, Hui Zhou, Wenpei Wang, Minmin Xia, Jing Wang, Qi. Tang, Lin Chen, WDM-RoF-PON architecture for flexible wireless and wire-line layout, j. Opt. Commun. Netw 2 (2) (2010) 117.

[8] Hyun-Seung Kim, Thang Tien Pham, Yong-Yuk Won, Ang-Kook Han, Simultaneous wired and wireless 1.25-Gb/s bidirectional WDM-RoF transmission using multiple optical carrier suppression in FP LD, J. Lightwave Technol. 27 (14) (2009) 2744.

[9] Yikai Su, Xiangqing Tian, Indra Widjaja, Weisheng Hu, Lilin Yi, Peigang Hu, Yi. Dong, Hao He, Optical VPN in PON using TDM-FDM signal format, Proc. OFC, 2006,, paper OTuJ5.

[10] Yue Tian, Yikai Su, Lilin Yi, Lufeng Leng, Xiangqing Tian, Hao He, Xinyu Xu, Optical VPN in PON based on dpsk erasing/rewriting and DPSK/IM formatting using a single Mach–Zehnder modulator, Proc. ECOC, 2006,, Tu4.5.6.

[11] Y. Su, P. Hu, W. Hu, J. Zhang, L. Leng, H. He, X. Tian, Y. Jin, A packet-switched waveband-selective PON enabling optical internetworking among ONUs, Proc. ECOC, 2005,, paper We4.P95.

[12] Jianjun Yu, et al., Demonstration of a novel WDM passive optical network architecture with source-free optical network units, IEEE Photon. Technol. Lett. 19 (8) (2007) 571.

[13] Yue Tian, Tong Ye, Yikai Su, Demonstration and scalability analysis of all-optical virtual private network in multiple passive optical networks using ASK/FSK FORMAT, IEEE Photon. Technol. Lett. 19 (20) (2007) 1595.

[14] P.F.M. Smulders, 60 GHz radio: Prospects and future directions, Proc. IEEE Benelux Chapter on Communications and Vehicular Technology, Eindhoven, The Netherlands, 2003, p. 1.

[15] A.H. Gnauck, P.J. Winzer, Optical phase-shift-keyed transmission, J. Lightwave Technol. 13 (1) (2005) 116.

[16] Z. Jia, J. Yu, G.K. Chang, A full-duplex radio-over-fiber system based on optical carrier suppression and reuse, IEEE Photon. Technol. Lett. 18 (16) (2006) 1726.